Supplemental figures.

Sup. Figure 1. Purity of transferred NKT cells

(A) The purity of sorted NKT from indicated donors, including NKT cells from mock-infected mice (WT NKT), from H3N1-infected mice (vNKT), from Vα14 Tg (Vα14 NKT), from PI57-treated mice (PI57-NKT) or from α-GalCer-treated BALB/c (α-Gal-NKT), was assessed by FACS.

(B) The sorted NKT cells from WT (WT NKT) and Vα14 Tg (Vα14 NKT) mice were assessed by FACS for $CD4^+$, DN NKT cell subsets or for contamination by T_{Reg} cells ($CD4^+CD25^+Foxp3^+$).

(C) The sorted NKT cells from H3N1 infected suckling mice 42 days after infection were assessed by FACS for $CD4^+$, DN NKT cell subsets.

Sup. Figure 2. TLR7 and T-bet affect cytokine productions of H3N1 exposed NKT cells in lung.

2 wk-old WT, $TLR7^{-/-}$ or $T\text{-}bet^{-/-}$ mice were infected by H3N1 or mock-infected. Lung cells were harvested on day 1, day 14 (**A**), or day 42 (**B, C, D**) post-infection.

(A) The percentage of IFN-γ or IL-4 secreting $CD4^+$ NKT and DN NKT subsets in WT or $T\text{-}bet^{-/-}$ mice 1 or 14 days post-infection were assessed by FACS.

(B)-(D) Lung cells were harvested on day 42 after infection and stimulated ex vivo with 10 or 100 ng/ml α-GalCer or vehicle for 96 hrs. Concentration of IFN-γ (**b**) and IL-4 (**c**) in the supernatant was measured by ELISA. *p<0.05,***p<0.001, compared to mock or wt group.

(D) Ratio of IFN-γ/IL-4 secretion from NKT with 100ng/ml α-GalCer was calculated. ***p<0.001, compared to the mock group.

(E) The total RNA from H3N1-infected WT or $T\text{-}bet^{-/-}$ mice lungs was isolated on day 42, and analyzed by QRT-PCR for IL-13 or IL-17 mRNA expression. *p<0.05, ***p<0.001, compared to the mock group.

Sup Figure 3. Treatment of 2 wk-old mice with α-GalCer did not prevent OVA induced AHR.

(A) NKT from α-GalCer or vehicle-treated mice were adoptively transferred to OVA-sensitized
BALB/c recipients. AHR was measured after OVA challenge.

(B) $T\text{-}bet^{-/-}$ mice (n=4-6 per group) received 50 μg PI57 or vehicle at 2 wks of age. After sensitization and challenge with OVA, AHR was measured on day 44. The protective effect of PI57 depends on T-bet expression.

Sup Figure 4. ^{1}H, ^{13}C NMR spectrometry, TLC analysis, ES-mass spectrometry of lipids from *H. pylori* SS1, a human *H. pylori* S strains and synthetic PI57 lipid.
(A) ES-MS negative mode spectrum of AGlc-Chol lipid.
(B) 1H NMR spectrum of AGlc-Chol lipid recorded in CDCl3-CD3OD (2:1, v/v) at 300K (500.13 MHz).
(C) Two-dimensional 1H -1H COSY NMR spectrum of AGlc-Chol lipid recorded in CDCl3-CD3OD (2:1, v/v) at 300K (500.13 MHz).
(D) 1H NMR spectrum of synthetic PI57 lipid recorded in CDCl3-CD3OD (2:1, v/v) at 300K (300 MHz).

Supplemental Material and Methods

Lung and spleen cells isolation. Whole lungs were flushed with PBS injected into the right ventricle, removed, and rinsed in PBS. The lungs were then diced on a wax board before incubating in 9.6 ml of RPMI 1640 medium with 0.1% DNase I (fraction IX; Sigma-Aldrich) and 1.6 mg/ml collagenase (CSL4; Worthington Biochemicals) at 37^{o}C on an orbital shaker for 30 min. The digest was passed multiple times through an 18-gauge needle and allowed to incubate for another 30 min before filtered. RBC were removed by 4-min incubation in lysis buffer (Sigma-Aldrich) at room temperature. Single-cell suspensions of spleen lymphocytes were obtained by mechanical disruption and RBC lysis.

Flow cytometry. Cells were preincubated with anti-Fcγ blocking mAb (2.4G2) and washed before staining. Cells were stained with anti-mouse PE-Texas red-conjugated CD45, PeCy5.5-conjugated CD25, Alexa Fluor 700-conjugated CD8 mAb, and Alexa Fluor 750-conjugated CD4 mAb (clone RM4-5). NKT cells were identified using APC-conjugated TCRβ (clone H57-597; eBioscience) and PE-conjugated, PBS57-loaded, CD1d-tetramers (with empty CD1d tetramers always used as control). Tetramers were provided by the NIAID Major Histocompatibility Complex Tetramer Core Facility, Atlanta, GA. For intracellular staining, after permeabilization (Cytofix/Cytoperm kit; BD Biosciences), cells were incubated with FITC-conjugated IL-4, FITC-conjugated IFN-γ, or the respective isotype control antibodies, FITC-conjugated rat IgG1κ (eBioscience). Cells were analyzed on a BDCanto flow cytometer (BD Biosciences) using FlowJo 8.3.3 software (Tree Star, Inc.).

Histopathologic analysis. The lungs were taken from mice, infused with 10% formalin and embedded in paraffin. Lung sections were cut (5 μm thick) and stained with hematoxylin/eosin (HE) for optic microscopy examination.

Mouse and human NKT cell lines. To establish mouse NKT cell lines, NKT cells were purified by a two-step sorting strategy using MACS. Spleen cells from BALB/c or BALB/c Vα14Jα18 Tg mice were depleted of T cells, B cells, granulocytes, macrophages and DCs by AutoMacs, then stained with PE conjugated-CD1d tetramer and FITC conjugated-anti-TCRβ mAb, and sorted using a MoFlo cell sorter (Dako). The purity of the sorted cells was >99%. To propagate the cells, sorted NKT cells were cultured in 96-well flat-bottom plates (1 X 10^5 cells/well) with 5 X 10^3 bone-marrow derived DC in the presence of murine IL-15 (Pepro Tech). Cells were subcultured and restimulated with fresh DCs once a week.
Human NKT cells were isolated from peripheral blood of normal volunteers,using a PE-conjugated anti-human NKT cell antibody (clone 6B11, which recognizes the CDR3 loop of the conserved Vα24 TCR found on *i*NKT cells) (BD Pharmingen) and anti-PE MACS beads (Miltenyi Biotec). Cells retained on the MACS column were then eluted. $CD14^+$ cells were obtained using anti-CD14 MACS beads and differentiated into dendritic cells (DCs) by culture with GM-CSF (2.5μg/ml) and rIL-4 (2μg/ml) for 1 wk. NKT cells and DCs (ratio 10:1) were co-cultured in RPMI 1640 medium containing 10% FCS, 100 U/ml rIL-2 (R&D Systems) and 1ng/ml rIL-15 (Peprotech).
Mouse NKT cell hybridomas. NKT cell hybridomas were established from C57BL/6 thymic NKT cells by fusion with thymoma BW5147 as previously describes (1)

Stimulation of invariant Vα14 NKT cell hybridomas with glycolipids coupled with immobilized CD1/β2m proteins. Culture wells were coated with recombinant CD1/β2m dimer proteins (Becton Dickinson) according to the manufacture's protocols. Cholesteryl glycosides dissolved in DMEM were added to the well, incubated for 1 day at 4 C, and then washed with DMEM. Hybridomas derived from invariant Vα14 NKT cells and an irrelevant $Vβ8^+$ T cell as a control (1) were cultured for 1 day in the wells. Cytokines in the culture supernatants were determined by ELISA.

Human NKT cell clone. CD1d transfected K562 cells and CD1d restricted human NKT cell clone BM2a.3 were previously described (2). The anti-CD1d antibody (clone 12.1.1.1) experiments have been performed as described (3).

In vitro culture of human NKT cell clone with CD1d coated plates. Maxisorp plates (Nunc) were coated with PBS diluted recombinant human CD1d/β2 microglobulin Fc fusion proteins (0.5μg/well; kindly provided by Dr. Jenny Gumperz (4) and anti-LFA-1 antibodies (0.05μg/well, AbD Serotec) overnight at 4^0C. After washing with PBS, immobilized CD1d was loaded with sonicated lipid antigens diluted in 25% DMSO/dH_2O by overnight incubation at 37^0C. After washing with PBS and culture media, NKT cells were added (5 x 10^4 cells/well) and culture supernatants were analyzed for IFN-γ by ELISA after overnight culture at 37^0C.

Helicobacter pylori

Bacterial strains and growth conditions: *Helicobacter pylori* SS1 mouse strain and as described earlier isolate 17B/RH of human *H. pylori* S form strain (5) were grown on solid agar plates with 7% horse blood, at 37°C under microaerobic conditions (5% O_2, 10% CO_2 and 85% N_2).

Knockout of Hp0421 glucosyltransferase.

Hp0421 was first amplified by PCR from *H. pylori* genomic DNA using the primers Hp0421-F (5'-ATG GTT ATT GTT TTA GTC GTG-3') and Hp0421-R (5'-TTA TGA TAA GGT TTT AAA GAG-3'), and the PCR product was subsequently cloned into SmaI-digested pUC19. The resultant plasmid was then linearised using a unique BglII site in the Hp0421 sequence, and BamH1-cut Cm-resistance cassette was cloned into this BglII site. The pUC18 cloned Hp0421 gene was thus disrupted at bp position 809 by the CmR cassette. The resultant allelic exchange plasmid pUC18-Hp0421::CmR was then introduced into *H. pylori* by natural transformation. *H. pylori* were inoculated on an agar plate on areas of 10-15 mm in diameter, and incubated for 7 hours, 37°C, microarobic. Aliquots of plasmid pUC19 with insert Hp0421::CmR were spotted directly onto the inoculated agar, (0,7 μg in 7 μl), and incubation was continued overnight.

The bacteria were harvested in 1 ml PBS, pelleted and resuspended in 100 μl PBS and were spread on blood agar plate with chlooramphenicol 25 g/ml to select transformants.

After incubation for 5 days, single colonies were taken and grown up.

Disruptants were confirmed by PCR using the primers F (5'-GAGGGAATGATAGAAATTG-3') and R (5'-TCCCATAATCATGGACTTC-3'); bonafide mutants yielded a band of size 1.8 kb, 1.1 kb expected from the wild type strain. More details of experiments can be found in paper (6).

Lipid Extraction and Purification.

To extract polar lipids, 20 ml of $CHCl_3$, CH_3OH (2:1, v/v) was added to the *H. pylori* pellets and the suspension was stirred for 6 h. Supernatant was removed and the pellets were re-extracted twice with 15 ml of $CHCl_3$, CH_3OH (2:1, v/v). The combined organic phases were concentrated and the lipids were re-extracted by Folch method. The lipid extract was dissolved in 15 ml of Folch low phase and washed three times with 4 ml of upper phase.

The final purification of the individual glycolipids was achieved by silica gel (Fluka, 60 mesh) column chromatography using stepwise gradient of chloroform/methanol (40:1 to 4:1, v/v).

The lipid extract was examined by TLC on aluminum-backed plates of silica gel 60 F_{254} (Merck 5554), using $CHCl_3$, CH_3OH, H_2O (65:25:4, v/v/v) or $CHCl_3$, CH_3OH (6:1, v/v). Glycolipids were visualized by spraying plates with α-naphthol/sulfuric acid followed by gentle charring of plates. Other types of lipids were visualized by spraying with 5% ethanolic molybdophosphoric acid and charring, or by using a Dittmer and Lester reagent that is specific for phospholipids.

NMR analysis. Deuterated solvents were from Aldrich. Glycolipids NMR spectrum were recorded in $CDCl_3$ - CD_3OD (2:1, v/v). NMR spectra were recorded on a Bruker DRX500 operating at 500.13 MHz for ^1H or Bruker AV300 operating at 300 MHz for ^1H. All spectra were run at 300 K. Data were acquired and processed using XWINNMR version 2.6 software on a Silicon Graphics work station. All two-dimensional NMR data were acquired nonspinning. Data points (2048) were used in acquisition for the fast domain (F2), and 512 points were used in the incremented domain (F1).

Mass spectrometic analysis. Glycolipids were dissolved in dichloromethane-methanol (2:1, v/v) and analyzed by Electrospray ionisation mass spectrometry (Micronos LCT) in positive or negative mode.

Results for Sup Figure 4.

After fractionation of lipid extracts from SS1 *H. pylori* and *H. pylori* S form by silica gel column chromatography, two major glycolipids were isolated. Glycolipid AGlc-Chol has the same R_f 0.49 for both H. *pylori* strains (TLC, chloroform-methanol (6:1, v/v) as well as MS-spectrum of positive mode ES-MS (781.9 $[M+Na]^+$ m/z) (not shown).

The second glycolipid Glc-Chol has equal for both strains R_f 0.26 (TLC, chloroform-methanol (6:1, v/v) as well as MS-spectrum of positive mode ES-MS (571. 4 $[M+Na]^+$ m/z) (not shown).

AGlc-Chol lipid ES-MS spectrum in negative mode showed an ion peaks at m/z 757.5 (sup. figure 4a) assignable to a $[M-H]^-$ and at m/z 547.3 assignable to a $[M-H]^-$ of glycolipid Glc-Chol. The difference in 210 Da between peaks corresponded the lost of myristic acid (C14:0) fragment.

These data are in agreement with reported for *H. pylori* cholesteryl glucosides (7). Indeed, ^{1}H NMR spectra of AGlc-Chols recorded in $CDCl_3$-CD_3OD (2:1, v/v) (500.13 MHz) were identical (sup. figure 4b and data not shown) and in agreement with cholesteryl-6-O-tetradecanoyl-α-glucopyranoside structure.

Based on the assignment of AGlc-Chol ^{1}H -^{1}H COSY NMR and proton coupling constants we confirmed the alpha configuration of glucopyranose with fatty acid substitution at position 6 (sup. figure 4c). The small $J_{1,2}$ coupling constant (3.84 Hz) of H-1 at 4.82 ppm indicated an α-anomeric configuration. The large coupling constant of H-2 (dd) at 3.36 ppm $J_{2,3}$ (9.52 Hz), H-3 (t) at 3.56 ppm $J_{3,4}$ (9.52 Hz) correlates with gluco-configuration of sugar. The downfield shift of H-6 (dd) at 4.08 ppm and H-6' (dd) at 4.38 ppm protons indicates that fatty acid esterifies the 6 position of glucose. Altogether, these data indicate cholesteryl-6-O-tetradecanoyl-α -glucopyranoside structure.

Compound PI57, the synthetic analog of AGlc-Chol, has near identical ^{1}H NMR spectrum to the natural glycolipid AGlc-Chol (recorded in $CDCl_3$-CD_3OD (2:1, v/v) (300.0 MHz) (sup. figure 4d).

The ^{1}H NMR spectrum of Glc-Chol and its synthetic analog PI56 corresponds to cholesteryl-α-glucopyranoside (7) (data not shown).

References*:*

1. Shimamura, M., Ohteki, T., Beutner, U., and MacDonald, H.R. 1997. Lack of directed V alpha 14-J alpha 281 rearrangements in NK1+ T cells. *Eur J Immunol* 27:1576-1579.
2. Brigl, M., van den Elzen, P., Chen, X., Meyers, J.H., Wu, D., Wong, C.H., Reddington, F., Illarianov, P.A., Besra, G.S., Brenner, M.B., et al. 2006. Conserved and heterogeneous lipid antigen specificities of CD1d-restricted NKT cell receptors. *J Immunol* 176:3625-3634.
3. Exley, M., Garcia, J., Balk, S.P., and Porcelli, S. 1997. Requirements for CD1d recognition by human invariant Valpha24+ CD4-CD8- T cells. *J Exp Med* 186:109-120.
4. Gumperz, J.E., Miyake, S., Yamamura, T., and Brenner, M.B. 2002. Functionally distinct subsets of CD1d-restricted natural killer T cells revealed by CD1d tetramer staining. *J Exp Med* 195:625-636

5. Bukholm, G., Tannæs, T., Nedenskov, P., Esbensen, Y., Grav, H. J., Hovig, T., Ariansen, S., and Guldvog, I.. 1997. Colony variation of *Helicobacter pylori*: pathogenic potential is correlated to cell wall lipid composition. *Scand. J. Gastroenterol.* 32:445-454.
6. Lebrun, A.H, Wunder,C., Hildebrand, J., Churin, Y., Zähringer, U., Lindner, B., Meyer, T.F., Heinz, E., and Warnecke, D.. 2006 Cloning of a cholesterol-alpha-glucosyltransferase from Helicobacter *pylori*. *J. Biol. Chem.* 281, 27765-27772.
7. Hirai, Y., Haque, M., Yoshida, T., Yokota, K., Yasuda, T., and Oguma, K.. 1995. Unique cholesteryl glucosides in *Helicobacter pylori*: composition and structural analysis. *J.Bacteriology,* 177, 5327-33.

Supl. Fig. 1

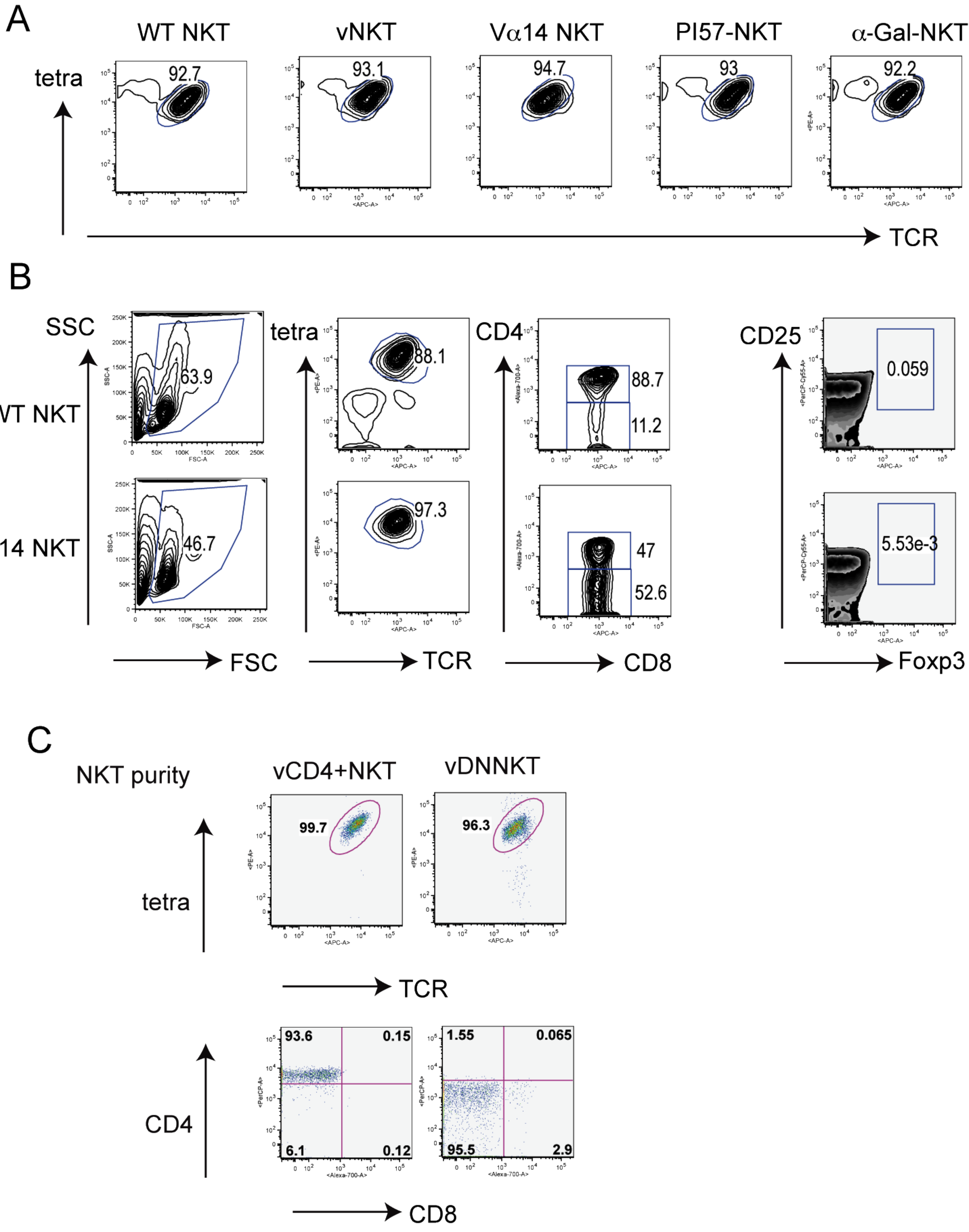
A
WT NKT
vNKT
Vα14 NKT
PI57-NKT
α-Gal-NKT
tetra
92.7
93.1
94.7
93
92.2
TCR
B
SSC
WT NKT
Vα14 NKT
63.9
46.7
FSC
tetra
88.1
97.3
TCR
CD4
88.7
11.2
47
52.6
CD8
CD25
0.059
5.53e-3
Foxp3
C
NKT purity
vCD4+NKT
vDNNKT
tetra
99.7
96.3
TCR
CD4
93.6
0.15
6.1
0.12
1.55
0.065
95.5
2.9
CD8

Supl Fig. 2

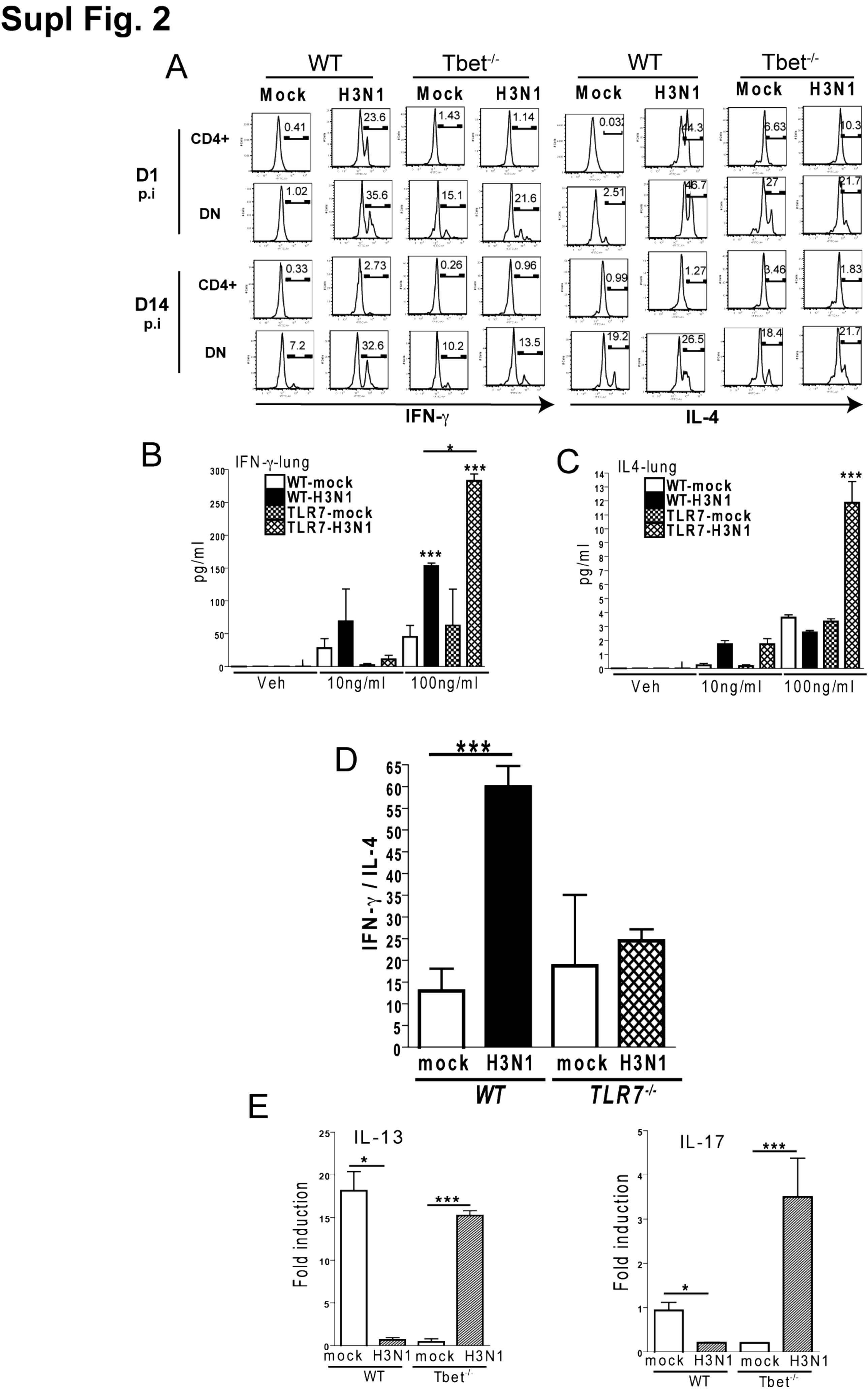
A
WT
Tbet-/-
WT
Tbet-/-
Mock
H3N1
Mock
H3N1
Mock
H3N1
Mock
H3N1
D1 p.i
CD4+
DN
D14 p.i
CD4+
DN
0.41
23.6
1.43
1.14
0.03
14.3
6.63
10.3
1.02
35.6
15.1
21.6
2.51
46.7
27
21.7
0.33
2.73
0.26
0.96
0.99
1.27
3.46
1.83
7.2
32.6
10.2
13.5
19.2
26.5
18.4
21.7
IFN-γ
IL-4
B
IFN-γ-lung
WT-mock
WT-H3N1
TLR7-mock
TLR7-H3N1
pg/ml
300
250
200
150
100
50
0
*
***
***
Veh
10ng/ml
100ng/ml
C
IL4-lung
WT-mock
WT-H3N1
TLR7-mock
TLR7-H3N1
pg/ml
14
13
12
11
10
9
8
7
6
5
4
3
2
1
0
***
Veh
10ng/ml
100ng/ml
D
***
IFN-γ / IL-4
65
60
55
50
45
40
35
30
25
20
15
10
5
0
mock
H3N1
mock
H3N1
WT
TLR7-/-
E
IL-13
Fold induction
25
20
15
10
5
0
*
***
mock
H3N1
mock
H3N1
WT
Tbet-/-
IL-17
Fold induction
5
4
3
2
1
0
*
***
mock
H3N1
mock
H3N1
WT
Tbet-/-

Supl Fig. 3

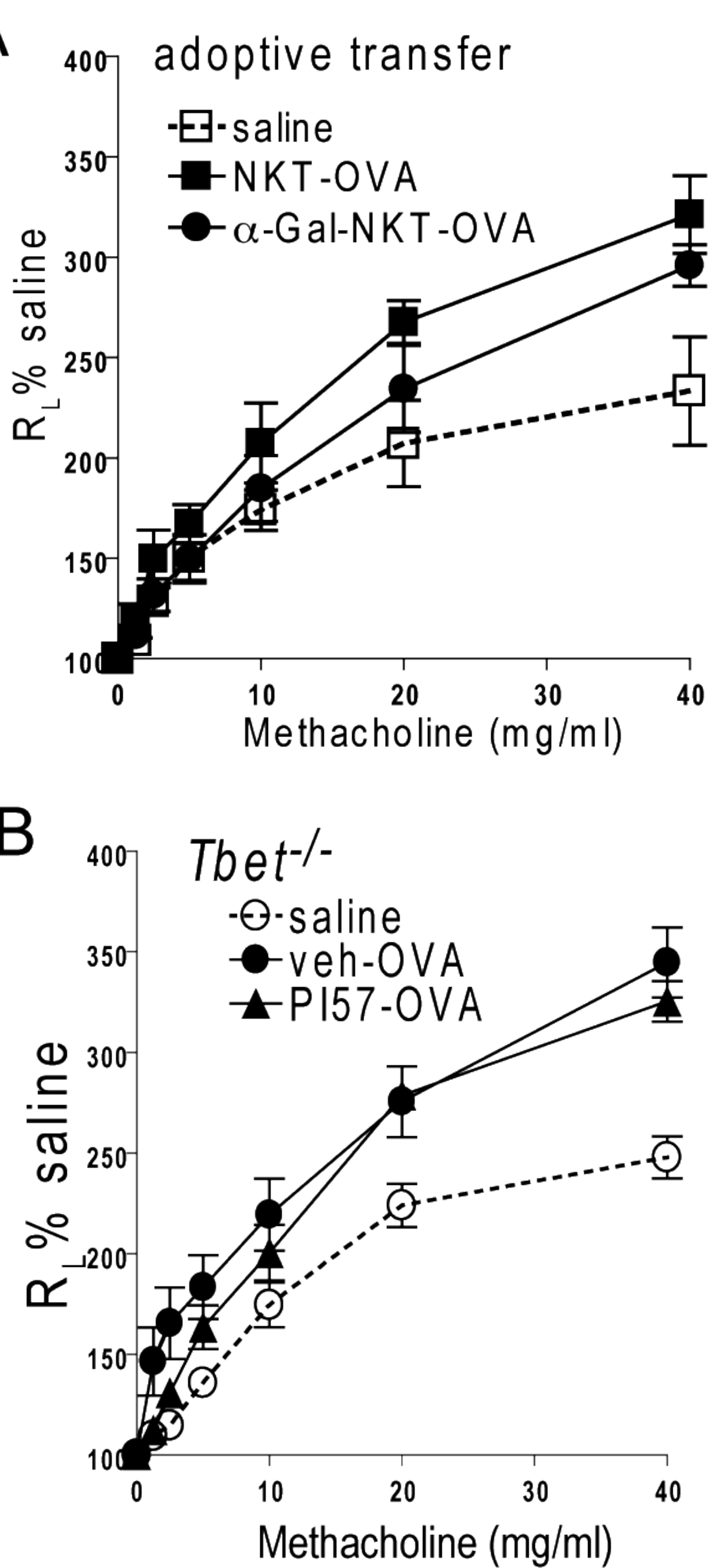
A
adoptive transfer
saline
NKT-OVA
α-Gal-NKT-OVA
R_L% saline
400
350
300
250
200
150
100
0
10
20
30
40
Methacholine (mg/ml)
B
Tbet-/-
saline
veh-OVA
PI57-OVA
R_L% saline
400
350
300
250
200
150
100
0
10
20
30
40
Methacholine (mg/ml)

Sup. Fig. 4

A

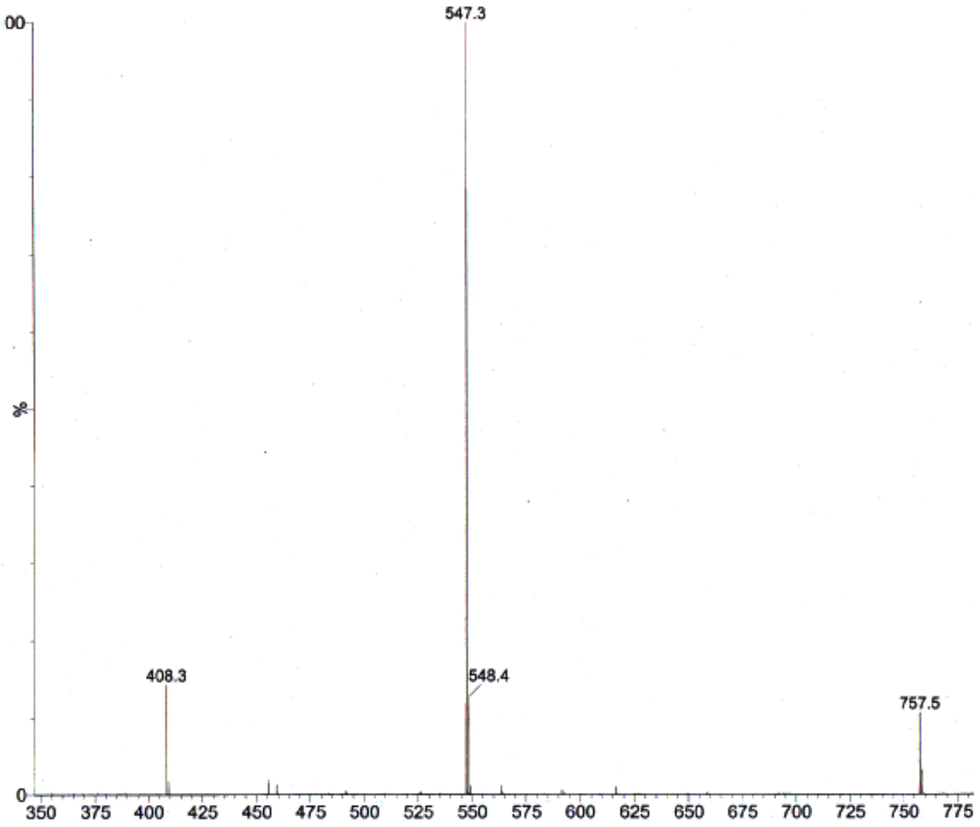

B

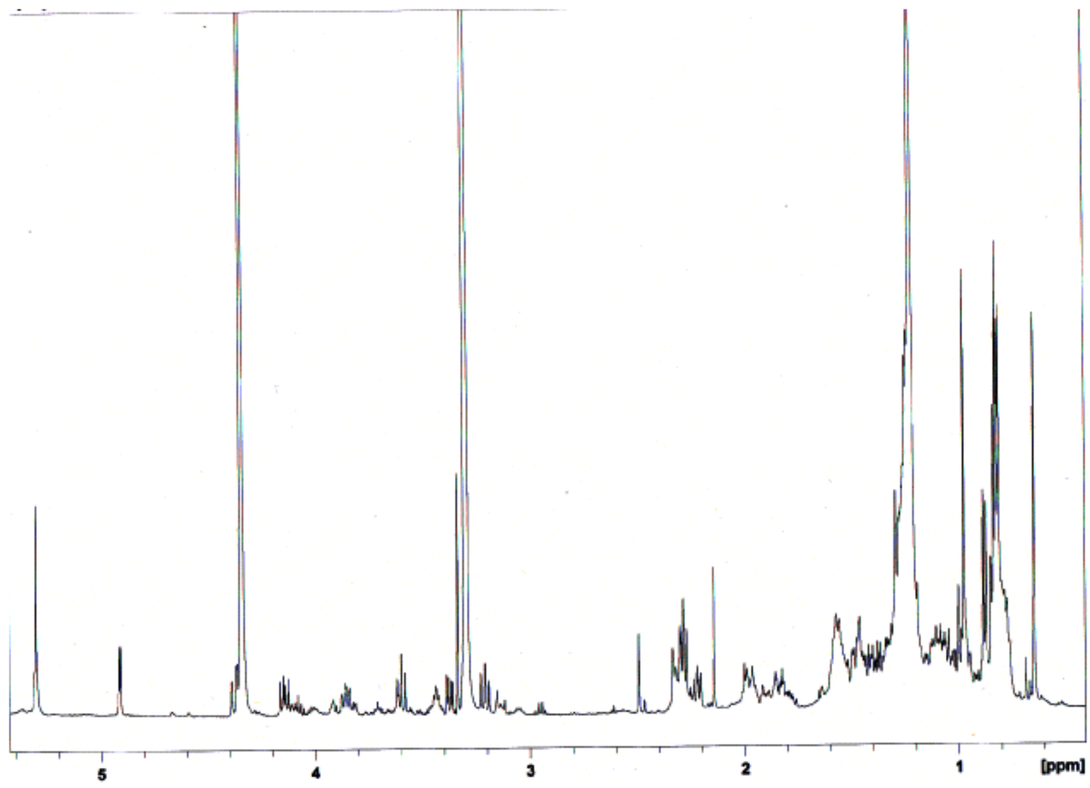

C

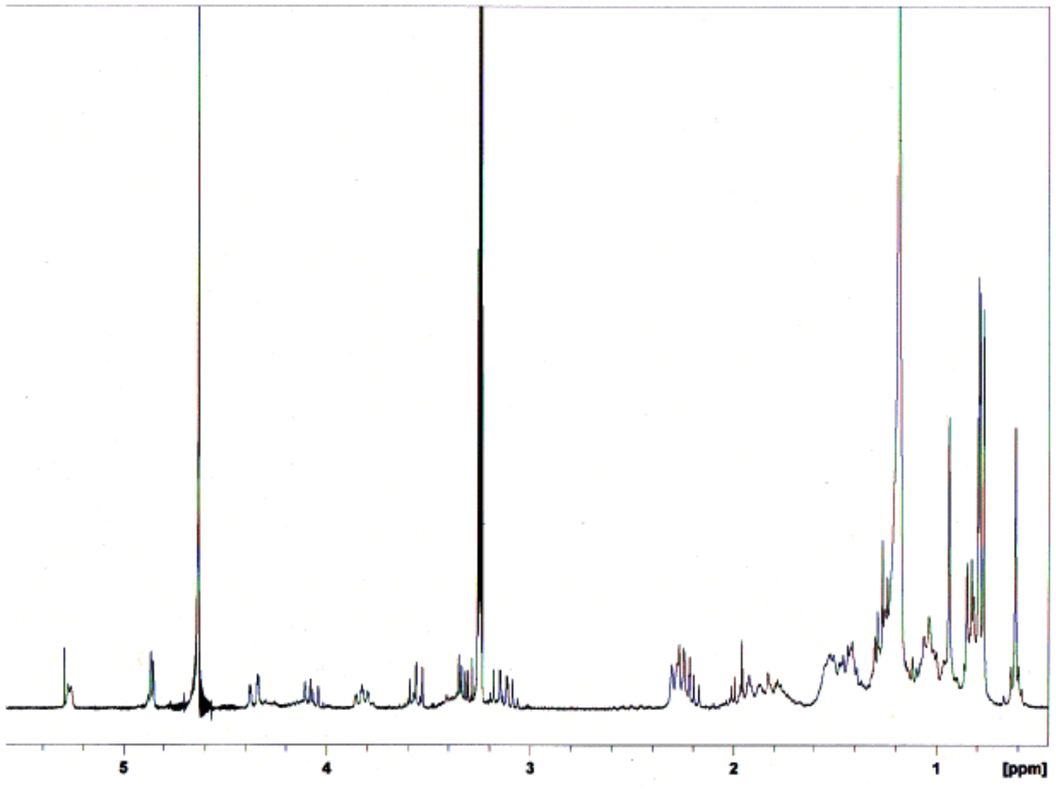

D